# 1,2-Metallotropic Shifts in Trimethylplatinum(IV) and Tricarbonylrhenium(I) Halide Complexes of Pyridazine and 4-Methylpyridazine†

**Edward W. Abel,[a] Elizabeth S. Blackwall,[a] Peter J. Heard,[a] Keith G. Orrell,*[,a] Vladimir Šik,[a] Michael B. Hursthouse,[b] Mohammed A. Mazid[b] and K. M. Abdul Malik[b]**

[a] *Department of Chemistry, The University, Exeter EX4 4QD, UK*

[b] *School of Chemistry and Applied Chemistry, University of Wales, College of Cardiff, Cardiff CF1 3TB, UK*

Pyridazine (pydz) and 4-methylpyridazine (4Me-pydz) form stable bis(monodentate) complexes of general formulae *fac*-$[PtXMe_3L_2]$ (X = Cl, Br or I) and *fac*-$[ReX(CO)_3L_2]$ (X = Cl, Br or I). These complexes in above-ambient temperature solutions exhibit 1,2-fluxional shifts between the nitrogen donor pairs of each ring. All linkage isomers of the pydz complexes are equivalent whereas three NMR-distinct linkage isomers, namely (1,1), (1,2)/(2,1) and (2,2) species, occur in solutions of the 4Me-pydz complexes. Fluxional exchange kinetics have been measured by variable-temperature $^1H$ NMR bandshape analysis and two-dimensional exchange spectroscopy (EXSY). Platinum-195 NMR data have been obtained for the complexes $[PtXMe_3(4Me\text{-}pydz)_2]$ (X = Br or I) and their fluxional dynamics investigated by $^{195}Pt$ two-dimensional EXSY and total bandshape analysis. Energy barriers, $\Delta G^{\ddagger}$ (298.15 K) for the 1,2-M–N fluxion are in the ranges 69–74 kJ mol$^{-1}$ for the $Pt^{IV}$ complexes and 84–90 kJ mol$^{-1}$ for the $Re^{I}$ complexes. The crystal structure of $[PtClMe_3(pydz)_2]$ shows the *cis* pydz rings oriented in a propeller arrangement with their unco-ordinated nitrogens oriented away from the *cis* positioned chlorine.

Six-membered aromatic nitrogen heterocycles (azines) represent an important class of ligand in co-ordination chemistry.[1] Azines possess relatively low energy $\pi^*$ orbitals, which act as good metal d-orbital electron acceptors making them strong ligands for d-electron rich transition-metal moieties such as platinum. Despite literature reports on the synthesis of a wide variety of transition-metal complexes of pyridazine (pydz) and its substituted analogues[2–4] and theoretical studies on the latent fluxionality of such complexes[5,6] we are aware of only three reported examples[7–9] of 1,2-metallotropic shifts between the nitrogen donors of these ligands, and in all three cases the studies of the intramolecular kinetics of the fluxional rearrangement were hampered by the presence of intermolecular ligand dissociation. Our group has now embarked on a systematic study of the fluxionality of 1,2-diazine complexes of transition metals. Pyridazine, 3-methylpyridazine (3Me-pydz), 4-methylpyridazine (4Me-pydz) and benzo[*c*]cinnoline (bzc) have been shown to undergo 1,2-metal–nitrogen shifts in tungsten pentacarbonyl complexes of type $[W(CO)_5L]$ (L = pydz, 3Me-pydz, 4Me-pydz or bzc) and precise energies of these movements have been evaluated by one- and two-dimensional NMR methods.[10]

This paper describes the fluxionality associated with bis(1,2-diazine) ligand complexes of transition metals. Two isoelectronic and isostructural series were chosen, namely the facial complexes of platinum(IV), *fac*-$[PtXMe_3L_2]$ (X = Cl, Br or I), and of rhenium(I), *fac*-$[ReX(CO)_3L_2]$ (X = Cl, Br or I), where, in both cases, L = pydz and 4Me-pydz. In such complexes 1,2-M–N shifts can occur in both diazine rings to produce chemically distinct or identical linkage isomers depending on the nature of the pyridazine. The fluxionality has been followed quantitatively by both $^1H$ and $^{195}Pt$ NMR spectroscopy, the main aims being to discover whether the 1,2 shifts in the adjacent *cis*-diazine rings occurred independently or by a concerted mechanism, whether there were any steric or electronic influences of the methyl substituent and, whether there was any dependence of the fluxion on the nature of the transition-metal moiety.

† *Supplementary data available:* see Instructions for Authors, *J. Chem. Soc., Dalton Trans.*, 1994, Issue 1, pp. xxiii–xxviii.

## Experimental

*Materials.*—The halogenotrimethylplatinum(IV) compounds $[(PtXMe_3)_4]$ (X = Cl, Br or I), were prepared by previous methods.[11,12] The compounds $[ReX(CO)_5]$ (X = Cl, Br or I) were also prepared by an earlier procedure.[13] Pyridazine and 4-methylpyridazine were purchased from Aldrich and Lancaster respectively and used as supplied.

*Synthesis of Complexes.*—All manipulations were performed under an atmosphere of dry oxygen-free nitrogen in freshly dried[14] and degassed solvents using standard Schlenk techniques.[15] The six complexes $[PtXMe_3L_2]$ (X = Cl, Br or I; L = pydz or 4Me-pydz) were synthesised in a similar way, as illustrated by the procedures for $[PtClMe_3L_2]$ (L = pydz or 4Me-pydz).

*Chlorotrimethylbis(pyridazine)platinum*(IV). Chlorotrimethylplatinum(IV) (0.30 g, 1.09 mmol, based on the monomeric unit) was dissolved in benzene (30 cm$^3$) and added to a stirred benzene solution (10 cm$^3$) of pyridazine (0.3 cm$^3$, 0.331 g, 4.13 mmol). The reactants were stirred at room temperature for *ca.* 18 h. The white solid formed was then filtered off and dried under vacuum. Purification was achieved by column chromatography using Florisil, and chloroform as the eluent. Recrystallisation from dichloromethane and hexane afforded 230 mg (48%) of the crystalline product.

*Chlorotrimethylbis-(4-methylpyridazine)platinum*(IV). 4-Methylpyridazine (0.5 g, 5.31 mmol) was added to a stirred solution of chlorotrimethylplatinum(IV) (0.60 g, 2.18 mmol, based on the monomeric unit) in benzene (30 cm$^3$). The

reactants were stirred at ambient temperature for *ca.* 18 h, after which time the volume was reduced to *ca.* 10 $cm^3$. Addition of hexane produced an off-white oil, which was stirred for 24 h in dichloromethane–hexane (20:80) to yield a waxy solid. This was dried by prolonged pumping *in vacuo* to yield the desired product (650 mg, 64.4%).

Full synthetic and analytical data for all the $[PtXMe_3L_2]$ complexes are given in Table 1.

The complexes $[ReX(CO)_3L_2]$ (X = Cl, Br or I, L = pydz; X = Br or I, L = 4Me-pydz) were prepared by the addition of the appropriate ligand to a solution of $[ReX(CO)_5]$ in chloroform using a method adapted from that reported for analogous pyridine complexes.[16] The preparation of $[ReCl(CO)_3(pydz)_2]$ is given as an illustrative example.

*Tricarbonylchlorobis(pyridazine)rhenium*(I). A mixture of $[ReCl(CO)_5]$ (0.32 g, 0.89 mmol) and pyridazine (1.0 g, 0.012 mol) in chloroform (20 $cm^3$) was heated under reflux for 5 h. The solvent was then removed under vacuum, and the resulting precipitate recrystallised from hot chloroform to give fine cream crystals (0.332 g, 81%).

Full synthetic and analytical data for all $[ReX(CO)_3L_2]$ complexes are given in Table 2.

*Physical Methods.*—Elemental analyses were carried out by Butterworth Laboratories, Teddington, Middlesex. Infrared spectra of the platinum(IV) complexes were recorded as CsI discs on a Nicolet Magna FT-IR spectrometer, equipped with a CsI beamsplitter, operating in the range 4000–200 $cm^{-1}$. Infrared spectra of the rhenium(I) complexes were recorded using matched $CaF_2$ solution cells on a Perkin Elmer model 881 spectrometer. Fast atom bombardment (FAB) mass spectra were obtained, courtesy of Dr. J. A. Ballantine, on a VG AutoSpec instrument using $Cs^+$ bombardment at 25 kV energy on the complexes dissolved in 3-nitrobenzyl alcohol. The NMR spectra were recorded on a Bruker AM250 or AC300 spectrometer operating at 250.12 or 300.12 MHz for $^1H$ studies. Platinum-195 NMR spectra were recorded on a Bruker AC300 spectrometer at 64.37 MHz. Spectra were recorded as $CDCl_3$, $(CDCl_2)_2$ or $CD_2Cl_2$–$C_6D_6$ solutions. Hydrogen-1 shifts are quoted relative to $SiMe_4$ as an internal standard and platinum-195 shifts relative to the absolute frequency scale $\Xi(^{195}Pt)$ = 21.4 MHz. NMR probe temperatures were varied using a standard B-VT unit calibrated against a digital thermometer (Comark). Temperatures are estimated to be accurate to ±1 °C. NMR band shape analyses employed the authors' version of the DNMR3 program.[17] Two-dimensional exchange spectroscopy (EXSY) was conducted using the Bruker NOESYPH automation program which produces the pulse sequence D1–90°–D0–90°–D9–90°-free induction decay. The relaxation delay D1 was set at 2 s, and the evolution time, D0

**Table 1** Synthetic and analytical data for the complexes *fac*-$[PtXMe_3L_2]$ (X = Cl, Br or I)

| X | L | Reaction time/h | Yield[a] (%) | ν(C–H)[b] $cm^{-1}$ | ν(Pt–C)[b,c] $cm^{-1}$ | ν(Pt–N)[b,c] $cm^{-1}$ | ν(Pt–X)[b] $cm^{-1}$ | Analysis[d] (%) C | H | N | $[M - X]^+/z$[e] |
|---|---|---|---|---|---|---|---|---|---|---|---|
| Cl | pydz | 18 | 48 | 2816.1s<br>2901.7s<br>2967.0s | 581.6w<br>582.4(sh) | 389.9m<br>423.6m | 237.9w | 30.6<br>(30.3) | 3.8<br>(3.9) | 12.9<br>(12.9) | |
| Br | pydz | 20 | 38 | 2812.5s<br>2904.4s<br>2966.9s | 580.0(sh)<br>581.1w | 388.4m<br>421.6m | | 27.6<br>(27.5) | 3.1<br>(3.6) | 11.4<br>(11.7) | |
| I | pydz | 20 | 47 | 2813.1s<br>2900.6s<br>2969.0s | 566.9w<br>577.2w | 386.7m<br>421.9m | | 25.2<br>(25.1) | 3.2<br>(3.3) | 10.9<br>(10.6) | |
| Cl | 4Me-pydz | 18 | 64 | 2816.8s<br>2898.9s<br>2963.0s | 549.2w | 394.0w | 242.9w | 33.0<br>(33.7) | 4.5<br>(4.6) | 11.4<br>(12.1) | 428 |
| Br | 4Me-pydz | 18 | 87 | 2817.0s<br>2896.3s<br>2963.4s | 549.0w | 399.0(sh)<br>400.8w | | 27.3<br>(30.7) | 3.5<br>(4.2) | 9.4<br>(11.0) | 428 |
| I | 4Me-pydz | 20 | 86 | 2820.5s<br>2901.4s<br>2964.8s | 548.5w<br>562.4w | 386.7w | | 26.6<br>(28.1) | 3.3<br>(3.8) | 8.8<br>(10.1) | 428 |

[a] Yields quoted relative to $[(PtXMe_3)_4]$. [b] Recorded as CsI discs: sh = shoulder, s = strong, w = weak. [c] Not all bands are resolved. [d] Calculated values in parentheses. [e] FAB mass spectral data.

**Table 2** Synthetic and analytical data for the complexes *fac*-$[ReX(CO)_3L_2]$ (X = Cl, Br or I)

| X | L | Reaction time/h | Yield[a] (%) | M.p./°C | ν(CO)[b]/$cm^{-1}$ | Analysis[c] (%) C | H | N |
|---|---|---|---|---|---|---|---|---|
| Cl | pydz | 5 | 81 | ≈235[d] | 2032, 1924, 1905 | 28.8<br>(28.6) | 1.9<br>(1.7) | 12.1<br>(12.1) |
| Br | pydz | 5 | 42 | ≈218[d] | 2029, 1920, 1904 | 26.4<br>(26.1) | 1.6<br>(1.6) | 10.9<br>(11.1) |
| I | pydz | 72 | 41 | ≈190[d] | 2030, 1925, 1908 | 24.3<br>(23.7) | 1.4<br>(1.5) | 10.1<br>(10.1) |
| Br | 4Me-pydz | 5 | 59 | ≈175[d] | 2029, 1924, 1905 | 29.5<br>(29.0) | 2.2<br>(2.3) | 10.3<br>(10.4) |
| I | 4Me-pydz | 80 | 47 | ≈165[d] | 2028, 1923, 1905 | 28.5[e]<br>(26.7) | 2.2[e]<br>(2.0) | 10.0[e]<br>(9.6) |

[a] Yields quoted relative to $[ReX(CO)_5]$. [b] Recorded in $CH_2Cl_2$. [c] Calculated values in parentheses. [d] Decomposition. [e] Slightly higher values due to an additional complex as detected in the $^1H$ NMR spectra.

had an initial value of $3 \times 10^{-6}$ s. For $^1$H two-dimensional EXSY spectra the mixing time D9 varied between 0.1 and 0.7 s according to the complex and experimental temperature. The frequency domains F1 and F2 each contained 1000 words of data. The spectral width was typically set at 250 Hz and the number of pulses at 16. For the $^{195}$Pt two-dimensional EXSY spectrum of $[PtIMe_3(4Me\text{-}pydz)_2]$ (see later), D1 was 2 s, D0 (initial) was $3 \times 10^{-6}$ s, the spectral widths in F1 and F2 frequency domains were 1126 and 2252 Hz respectively, and the mixing time D9 was 0.02 s. Rate data were extracted from the volume integrals of the $^1$H two-dimensional EXSY plots using the D2DNMR program described previously.[18]

*X-Ray Crystal Structure Determination.*—Crystals of $[PtClMe_3(pydz)_2]$ were prepared as described above and examined in Lindemann capillaries.

*Crystal data.* $C_{11}H_{17}ClN_4Pt$, $M = 435.816$, monoclinic, space group $P2_1/n$, $a = 8.555(2)$, $b = 12.210(2)$, $c = 13.403(1)$ Å, $\beta = 104.68(2)°$, $U = 1354.33$ Å$^3$, $Z = 4$, $D_c = 2.137$ g cm$^{-3}$, $F(000) = 824$, Mo-K$\alpha$ radiation, $\lambda = 0.710\,69$ Å, $\mu = 105.44$ cm$^{-1}$.

*Data collection and processing.* Data were obtained using a FAST TV area detector diffractometer situated at the window of a rotating anode generator, operating at 50 kV with a molybdenum anode as previously described.[19] The total number of reflections recorded was 6720, giving 3318 unique ($R_{int} = 0.052$).

*Structure analysis and refinement.* The structure was solved by Patterson methods and refined on $F_o^2$ using all 3318 unique data corrected for absorption. All non-hydrogen atoms were assigned anisotropic thermal parameters. The hydrogen atoms were inserted in calculated positions; the $U_{iso}$ values of the ring hydrogens were refined freely but those on the methyl groups were set at 1.5 times the $U_{eq}$ of the parent atom. The final $wR_2$ and conventional $R_1$ values based on the refinement using 165 parameters and all 3318 data were 0.092 and 0.041 respectively. The corresponding values for the 2553 reflections with $I > 2\sigma(I)$ were 0.085 and 0.033 respectively. The weighting scheme used was $w = 1/\sigma^2(F_o^2)$. The positions of the uncoordinated nitrogens were unequivocally determined by comparing thermal parameter values from suitable refinements. The computer programs used are given in ref. 20. Additional material available from the Cambridge Crystallographic Data Centre comprises H-atom coordinates and thermal parameters.

## Results and Discussion

(*i*) $[PtXMe_3(pydz)_2]$ **1** (X = Cl, Br *or* I).—The infrared spectra of these complexes showed three bands in the CH stretching region, two Pt–C and Pt–N stretches and one Pt–X (X = Cl) stretch, all indicative of a facial octahedral geometry.[21-24] Synthetic, analytical and infrared data are given in Table 1.

The ambient-temperature $^1$H NMR spectra of the complexes in $CDCl_3$ exhibited some line broadening of the aromatic $^1$H resonances. This disappeared on cooling to *ca.* −20 °C to reveal well resolved signals. The case of $[PtClMe_3(pydz)_2]$ is illustrated in Fig. 1.

The aromatic region consisted of three main multiplets in an intensity ratio 1 : 1 : 2 assigned to hydrogens A, B and C/D (Fig. 2) of the pyridazine ring. Multiplets A and B were distinguished by the fact that A exhibited $^{195}$Pt satellites and was shifted to higher frequency by virtue of its proximity to the metal-coordinated nitrogen. The platinum–methyl region exhibited two signals, each with $^{195}$Pt satellites. Their intensity ratio allowed unambiguous assignment to the equatorial (*trans* N) and axial (*trans* X) signals. The relative positions of the axial and equatorial Pt–Me signals proved halogen dependent, but in all cases the axial signals exhibit smaller magnitudes of $^3J$(Pt–H) couplings compared to their equatorial counterparts. This may be attributed to the greater *trans* influence of halogen X,

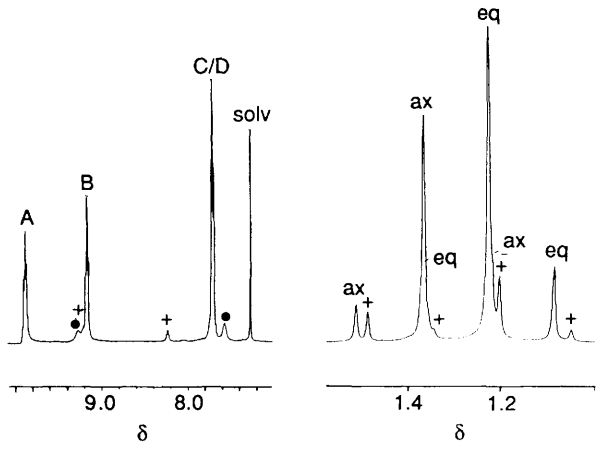


**Fig. 1** The $^1$H NMR spectrum (250 MHz) of $[PtClMe_3(pydz)_2]$ in $CDCl_3$ at 253 K. See Fig. 2 for labelling of main aromatic signals; solv = Solvent signal. Additional signals labelled + and • are due to the other complex species

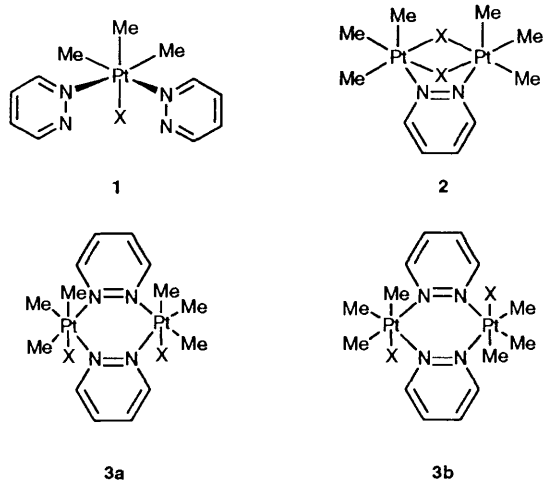


compared to a pyridazine ligand, causing a relative weakening and lengthening of the Pt–C(ax) bond. This is supported by the crystal structure of $[PtClMe_3(pydz)_2]$ (see later). Static NMR parameters for all three halide complexes are given in Table 3.

In addition to the main signals, due to complexes **1**, the $^1$H spectra of all three halide complexes contained additional signals, four in the aromatic region and two, with $^{195}$Pt satellites, in the Pt–Me region (see Fig. 1). These are attributed to small amounts of solution state dinuclear $Pt^{IV}$ complexes involving pyridazine as a bridging ligand, *viz.* $[(PtXMe_3)_2(pydz)]$ **2** and $[(PtXMe_3)_2(pydz)_2]$ **3a**, **3b**. Unfortunately, it has proved impossible to date to isolate these complex species or to characterise them further.

*Dynamic NMR studies.* On warming solutions of the complexes $[PtXMe_3(pydz)_2]$ the signals due to the aromatic hydrogens A and B exhibited dynamic broadening and eventual coalescence as a result of the 1,2-metallotropic shift. However, the spectra showed evidence of the additional complexes **2** and **3** being involved in an intermolecular exchange with the bis(pyridazine) complexes **1** in a similar temperature range thus frustrating attempts to measure rates of the intramolecular 1,2-shift process by band-shape analysis. However, rates of the 1,2-shift process were able to be measured by two-dimensional EXSY experiments at temperatures where the specifically intermolecular exchange was of negligible rate on the NMR chemical shift time-scale. This can be seen in the two-dimensional EXSY spectrum of $[PtClMe_3(pydz)_2]$ at 283 K (Fig. 3) where cross peaks due to the ring hydrogens A and B

**Table 3** Static $^1$H NMR parameters[a] for the complexes $[PtXMe_3(pydz)_2]$ (X = Cl, Br or I)

| | | | | δ(H)[c] | | |
|---|---|---|---|---|---|---|
| X | Solvent | T/K | δ(Pt–$CH_3$)[b] | A | B | C/D |
| Cl | $CDCl_3$ | 253 | 1.20(73.8)(eq) | 9.87 | 9.14 | 7.69 |
| | | | 1.35(70.8)(ax) | (AB ≈ 1)[d] | (AB ≈ 1)[d] | (AC ≈ 5)[d] |
| | | | | (AC ≈ 5)[d] | (BC ≈ 2)[d] | (AD ≈ 2)[d] |
| | | | | (AD ≈ 2)[d] | (BD ≈ 4.5)[d] | (BC ≈ 2)[d] |
| | | | | | | (BD ≈ 4.5)[d] |
| Br | $CDCl_3$ | 263 | 1.38(74.5)(eq) | 9.93 | 9.13 | 7.69 |
| | | | 1.43(71.0)(ax) | (AB = 1.1) | (AB = 1.1) | (AC = 4.8) |
| | | | | (AC = 4.8) | (BC = 3.0) | (AD = 3.0) |
| | | | | (AD = 3.0) | (BD = 5.0) | (BC = 3.0) |
| | | | | | | (BD = 5.0) |
| I | $CDCl_3$ | 253 | 1.43(71.5)(ax) | 10.0 | 9.13 | 7.70 |
| | | | 1.52(72.5)(eq) | (AB = 1.3) | (AB = 1.3) | (AC = 6.0) |
| | | | | (AC = 6.0) | (BC = 3.3) | (AD = 3.3) |
| | | | | (AD = 3.3) | (BD = 6.0) | (BC = 3.3) |
| | | | | | | (BD = 6.0) |

[a] Chemical shifts quoted relative to $SiMe_4$ as internal standard. [b] $^2J_{PtH}$/Hz given in parentheses; ax = axial, eq = equatorial. [c] See Fig. 2 for proton labelling; $^nJ_{HH}$/Hz given in parentheses; $J_{CD}$ not measurable. [d] Values uncertain due to poor resolution of the spectra.

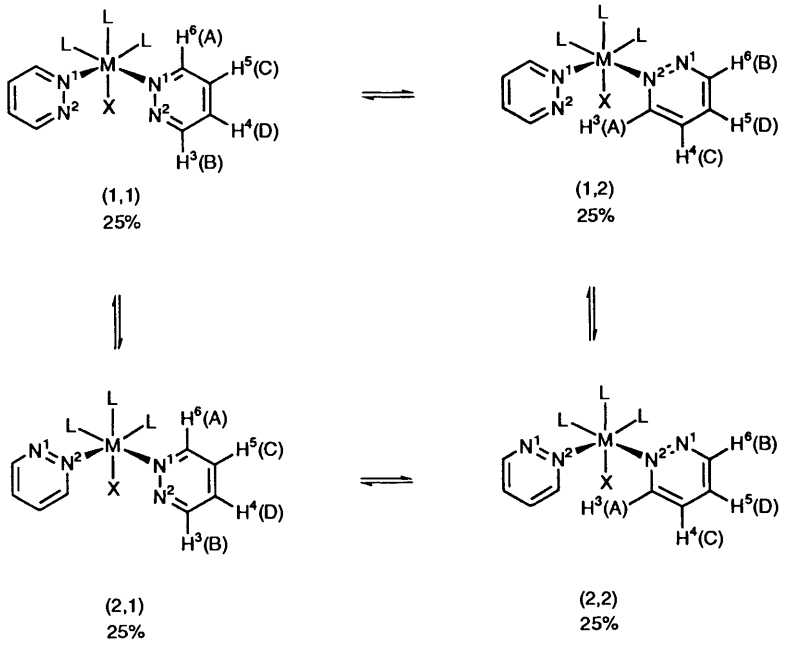


**Fig. 2** The degenerate set of linkage isomers (topomers) of the complexes *fac*-$[MXL_3(pydz)_2]$ showing the proton site exchange ABCD ⇌ BADC resulting from the 1,2 shift. The structures shown are arbitrarily chosen rotamers from the total set arising from rapid M–N bond rotations

are clearly seen whilst the additional signal due to the minor complex species displayed no cross peaks with A or B. Five two-dimensional EXSY experiments were carried out on each of the three complexes and accurate rates for the 1,2 shift deduced (Table 4).

The shift process, as depicted in Fig. 2, causes an interconversion between four species which are labelled according to which nitrogen atoms are metal-co-ordinated. If, however, metal–nitrogen bond rotation is fast on the NMR time-scale as appears apparent from the spectra, then all species are degenerate topomers since a 1,2-Pt–N shift on one ring is equivalent to a 180° rotation of that ring about the M–N bond. All species therefore have the same solution populations and give identical $^1$H NMR spectra. Nevertheless, exchange between pairs of species is detectable by one-dimensional bandshape analysis and two-dimensional EXSY by virtue of the ring proton site exchange ABCD ⇌ BADC.

Activation energy parameters for the 1,2 shift were calculated from the two-dimensional EXSY data and are given in Table 5. The Pt–Me region of the spectra was not sensitive to this fluxion, but at higher temperatures (> *ca.* 60 °C) the Pt–Me signals did display dynamic broadening due to the onset of axial–equatorial Pt–Me exchange arising from the well established scrambling process.[24]

*Crystal structure of* $[PtClMe_3(pydz)_2]$. This was obtained to confirm the facial octahedral geometry of the complexes and, in particular, to investigate the preferred orientations of the pyridazine rings. A view of the molecule with the atom numbering scheme is shown in Fig. 4. Fractional atomic coordinates are contained in Table 6, and all bond lengths and angles are given in Table 7. Little distortion from regular octahedral geometry is revealed. The adjacent pyridazine ligands open up the N(1)–Pt–N(3) angle to 91.3(2)°, so reducing the angles of the *trans* related bonds, namely N(1)–Pt–C(1) and N(3)–Pt–C(3) from 180° to 178.1(2) and 178.8(2)° respectively. The most interesting structural feature, however, is the orient-

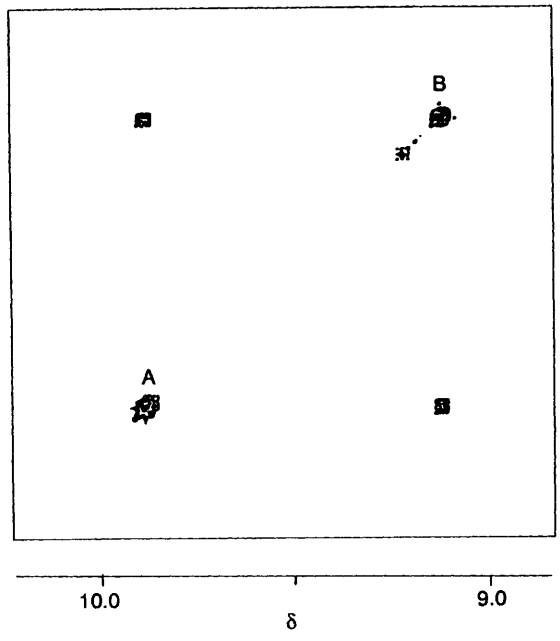


**Fig. 3** The $^1H$ two-dimensional EXSY NMR spectrum of $[PtClMe_3(pydz)_2]$ at 283 K showing the AB $\rightleftharpoons$ BA exchange due to the 1,2 shift. Additional signal without cross peaks is due to the minor complex species

ation of the pyridazine rings, both with respect to each other and to the $PtXMe_3$ moiety. It is apparent from Fig. 4 that the pyridazine rings are staggered with respect to each other in a propeller conformation with their ring planes approximately bisecting the Cl–Pt–C(3) and Cl–Pt–N(1) angles and their unco-ordinated nitrogens N(2) and N(4) oriented away from the chlorine atom. In this way non-bonded interactions both between the rings, and between the rings and the $PtClMe_3$ moiety, are minimised.

(*ii*) $[ReX(CO)_3(pydz)_2]$ (X = Cl, Br *or* I)—The static NMR data for the three halide complexes are given in Table 8. As expected the $^1H$ spectra are very analogous to the $Pt^{IV}$ complexes with corresponding ring hydrogen signals being displaced very slightly to higher frequencies. Chemical shift distinction between the A and B hydrogens is again large ($\Delta\delta$ = 0.6–0.9) whereas between hydrogens C and D it is very slight ($\Delta\delta$ = 0.01–0.02). There was no evidence of additional complex species involving bridging pyridazine ligands in contrast to the $Pt^{IV}$ complexes and the presence of the 1,2-metallotropic shift process could be monitored by one-dimensional NMR bandshape analysis. On warming the complexes to *ca.* 140 °C the A and B hydrogen multiplets displayed exchange broadening which was amenable to total bandshape analysis based on the spin exchange ABCD $\rightleftharpoons$ BADC. The case of $[ReCl(CO)_3(pydz)_2]$ is illustrated in Fig. 5. Some thermal decomposition of the complexes was apparent particularly at temperatures above *ca.* 100 °C, but this did not interfere with the bandshape analysis until *ca.* 140 °C. At least seven reliable rate constants for the process were measured for all three complexes and activation energy data calculated (Table 5).

(*iii*) $[PtXMe_3(4Me\text{-}pydz)_2]$ (X = Cl, Br *or* I).—Synthetic, analytical, infrared and mass spectral data for these complexes are reported in Table 1. It will be noted that the values for the C, H, N elemental analyses are substantially lower than the expected values. This is due to the presence of two other complexes, present in both the solid and solution states (see below), with bridging 4Me-pydz ligand(s), analogous to structures **2** and **3** earlier. These could not be separated from the main mononuclear complexes. FAB mass spectroscopy was therefore used to characterise further the mononuclear

**Table 4** Two-dimensional EXSY NMR data for $[PtXMe_3(pydz)_2]$ complexes

| X | *T*/K | Mixing time, D9/s | $k^*/s^{-1}$ |
|---|---|---|---|
| Cl | 303 | 0.15 | 4.98 |
| | 298 | 0.20 | 2.61 |
| | 293 | 0.35 | 1.20 |
| | 288 | 0.60 | 0.55 |
| | 283 | 0.70 | 0.28 |
| Br | 303 | 0.20 | 4.36 |
| | 298 | 0.25 | 2.70 |
| | 293 | 0.20 | 1.42 |
| | 288 | 0.55 | 0.55 |
| | 283 | 0.30 | 0.30 |
| I | 299 | 0.10 | 6.36 |
| | 293 | 0.15 | 2.28 |
| | 288 | 0.20 | 1.47 |
| | 278 | 0.45 | 0.19 |
| | 273 | 0.60 | 0.10 |

* First-order rate constants for the 1,2-shift process. Uncertainties are $\pm 0.02\ s^{-1}$.

**Table 5** Eyring activation parameters[a] for the complexes $[PtXMe_3(pydz)_2]$ and $[ReX(CO)_3(pydz)_2]$

| Complex | $\Delta H^‡$/kJ mol$^{-1}$ | $\Delta S^‡$/J K$^{-1}$ mol$^{-1}$ | $\Delta G^‡$/kJ mol$^{-1}$ |
|---|---|---|---|
| $[PtClMe_3(pydz)_2]$ | 103.1 ± 1.6 | *b* | 70.69 ± 0.03 |
| $[PtBrMe_3(pydz)_2]$ | 95.7 ± 5.2 | *b* | 70.8 ± 0.10 |
| $[PtIMe_3(pydz)_2]$ | 107.8 ± 5.8 | *b* | 68.7 ± 0.3 |
| $[ReCl(CO)_3(pydz)_2]$ | 84.9 ± 2.0 | 0.9 ± 5.5 | 84.6 ± 0.4 |
| $[ReBr(CO)_3(pydz)_2]$ | 97.0 ± 4.0 | 32.9 ± 10.6 | 87.2 ± 0.9 |
| $[ReI(CO)_3(pydz)_2]$ | 106.4 ± 4.9 | 57.4 ± 12.7 | 89.3 ± 1.1 |

[a] $\Delta G^‡$ quoted at 298.15 K. [b] Unreliable values due to narrow temperature range of measurement.

$[PtXMe_3(4Me\text{-}pydz)_2]$ species. However, the FAB mass spectra did not show any parent ion peaks, only a strong peak at $m/z$ = 428 in each case, corresponding to loss of halogen X. The observed isotope pattern was consistent with that predicted for the species $[PtMe_3(4Me\text{-}pydz)_2]^+$, *i.e.* $[M - X]^+$. Weak, higher-mass peaks were also detected. These could possibly be attributed to the dinuclear complexes (see above).

The methyl substituent in the 4 position of the pyridazine rings destroys the $C_{2v}$ symmetry of the rings leading to different linkage isomers, defined in Fig. 6 as (1,1), (1,2), (2,1) and (2,2) according to which nitrogens are co-ordinated. Isomers (1,1), (1,2)/(2,1) and (2,2) are chemically distinct with (1,2) and (2,1) being enantiomers. On cooling solutions of these complexes to *ca.* 0 °C very complex $^1H$ spectra were obtained due to the presence of all four non-exchanging isomers and minor complex products. Spectra of solutions in $CDCl_3$, $CD_2Cl_2$ and $C_6D_6$ showed fewer than the predicted theoretical number of resonances (*viz* four ligand methyl, seven Pt–Me with $^{195}Pt$ satellites, and twelve aromatic hydrogen signals). However, in the case of $[PtClMe_3(4Me\text{-}pydz)_2]$ a judicious choice of mixed solvent ($CD_2Cl_2$–$C_6D_6$, 40:60 v/v) revealed the expected number of signals and allowed complete assignments in the ligand methyl and Pt–Me regions (Fig. 7). Signals were assigned on the assumptions that isomer populations are in the order (1,1) > (1,2) = (2,1) > (2,2) and ligand methyls will be more deshielded when $N^2$ rather than $N^1$ is co-ordinated. In the Pt–Me region the equatorial methyl signals will be shifted to lower frequency due to the *trans* influence of the pyridazine ligands. Three axial and four equatorial signals each with $^{195}Pt$ satellites were distinguished (Fig. 7) as theoretically predicted (Table 9). The aromatic region consisted of three groups of signals at δ 7.16–7.47, 8.76–9.28 and 9.92–10.21, which, although not fully assignable to individual isomers, could be attributed to the 5-, 3- and 6-position hydrogens respectively.

As in the case of the unsubstituted pyridazine complexes the

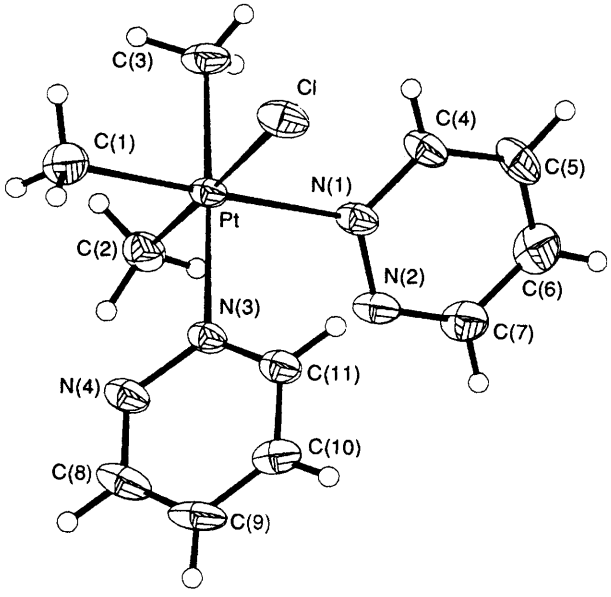


**Fig. 4** Crystal structure of $[PtClMe_3(pydz)_2]$ showing the atom labelling scheme

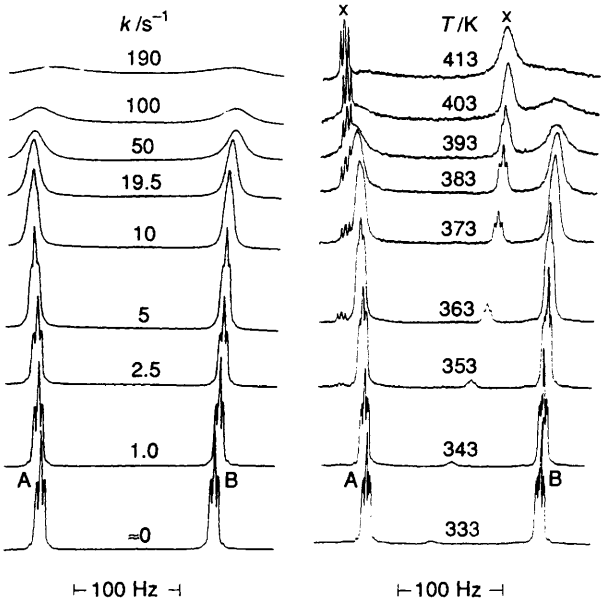


**Fig. 5** Variable-temperature $^1H$ NMR spectra and 'best-fit' computer simulations of $[ReCl(CO)_3(pydz)_2]$ showing the exchange of the A and B ring hydrogens. Signals denoted by X are due to a decomposition product

spectra also contained signals which are attributed to bridging pyridazine complexes analogous to structures **2** and **3**.

On warming the mixed solvent solution of the chloro complex changes occurred in all three spectral regions due to the onset of the 1,2-shift process. However, the close proximities of both the Pt–Me and ligand methyl signals and the presence of the additional complex species precluded any accurate quantitative DNMR studies (one-dimensional bandshape analysis or two-dimensional EXSY). An approximate value of the Gibbs free energy, $\Delta G^{\ddagger}$, for the fluxion was, however, obtained from a single two-dimensional EXSY experiment at 295 K.

Studies of the bromo and iodo complexes in $CD_2Cl_2$–$C_6D_6$ of varying proportions, however, did not yield sufficiently well resolved $^1H$ spectra for quantitative analysis. Dynamic data had to be sought, therefore, by other means. Platinum-195 spectra were accordingly investigated and found to be well

**Table 6** Fractional atomic coordinates ( $\times 10^4$) for $[PtClMe_3(pydz)_2]$

| Atom | *x* | *y* | *z* |
|---|---|---|---|
| Pt | 1512(1) | 2414(1) | 3159(1) |
| Cl | 4511(2) | 2433(1) | 3470(2) |
| N(1) | 1755(6) | 1537(4) | 4617(3) |
| N(2) | 870(6) | 1867(4) | 5248(4) |
| N(3) | 1626(6) | 3989(4) | 3937(3) |
| N(4) | 491(6) | 4729(4) | 3542(4) |
| C(1) | 1260(9) | 3184(6) | 1771(5) |
| C(2) | −988(9) | 2374(5) | 2885(6) |
| C(3) | 1373(8) | 954(5) | 2405(5) |
| C(4) | 2689(8) | 656(5) | 4842(5) |
| C(5) | 2771(8) | 30(5) | 5723(5) |
| C(6) | 1889(9) | 367(6) | 6351(5) |
| C(7) | 954(8) | 1293(6) | 6091(5) |
| C(8) | 593(9) | 5708(5) | 3988(5) |
| C(9) | 1771(8) | 6016(5) | 4825(5) |
| C(10) | 2902(8) | 5257(5) | 5225(5) |
| C(11) | 2804(8) | 4230(5) | 4763(5) |

**Table 7** Bond lengths (Å) and angles (°) for $[PtClMe_3(pydz)_2]$

| | | | |
|---|---|---|---|
| Pt–C(3) | 2.038(6) | Pt–C(1) | 2.047(6) |
| Pt–C(2) | 2.077(7) | Pt–N(3) | 2.178(5) |
| Pt–N(1) | 2.190(4) | Pt–Cl | 2.493(2) |
| N(1)–N(2) | 1.333(6) | N(1)–C(4) | 1.329(7) |
| N(2)–C(7) | 1.315(8) | N(3)–N(4) | 1.333(6) |
| N(3)–C(11) | 1.328(8) | N(4)–C(8) | 1.330(8) |
| C(4)–C(5) | 1.394(9) | C(5)–C(6) | 1.330(10) |
| C(6)–C(7) | 1.378(9) | C(8)–C(9) | 1.357(9) |
| C(9)–C(10) | 1.350(9) | C(10)–C(11) | 1.391(8) |
| | | | |
| C(3)–Pt–C(1) | 88.4(3) | C(3)–Pt–C(2) | 87.9(3) |
| C(1)–Pt–C(2) | 89.0(3) | C(3)–Pt–N(3) | 178.8(2) |
| C(1)–Pt–N(3) | 90.6(2) | C(2)–Pt–N(3) | 91.4(2) |
| C(3)–Pt–N(1) | 89.8(2) | C(1)–Pt–N(1) | 178.1(2) |
| C(2)–Pt–N(1) | 90.4(2) | N(3)–Pt–N(1) | 91.3(2) |
| C(3)–Pt–Cl | 91.1(2) | C(1)–Pt–Cl | 90.8(2) |
| C(2)–Pt–Cl | 179.0(2) | N(3)–Pt–Cl | 89.56(13) |
| N(1)–Pt–Cl | 89.69(13) | N(2)–N(1)–C(4) | 120.4(5) |
| N(2)–N(1)–Pt | 118.5(4) | C(4)–N(1)–Pt | 120.9(4) |
| C(7)–N(2)–N(1) | 117.9(5) | N(4)–N(3)–C(11) | 120.2(5) |
| N(4)–N(3)–Pt | 118.0(4) | C(11)–N(3)–Pt | 121.8(4) |
| C(8)–N(4)–N(3) | 118.2(5) | N(1)–C(4)–C(5) | 122.3(6) |
| C(6)–C(5)–C(4) | 116.8(6) | C(5)–C(6)–C(7) | 118.7(6) |
| N(2)–C(7)–C(6) | 123.8(6) | N(4)–C(8)–C(9) | 124.8(6) |
| C(10)–C(9)–C(8) | 116.5(6) | C(9)–C(10)–C(11) | 119.0(6) |
| N(3)–C(11)–C(10) | 121.2(6) | | |

suited in identifying the three types of linkage isomers. The $^{195}Pt$ spectra of the bromo and iodo complexes in $CDCl_3$ revealed three signals within a narrow chemical shift range of *ca.* 3 ppm. Their unambiguous assignment, however, posed some difficulty. This was resolved by a two-dimensional EXSY experiment performed at 308 K on the iodo complex at which temperature the 1,2-shift process produced cross peaks between adjacent pairs of signals only (Fig. 8). This information, when used in conjunction with the earlier isomer population arguments, provided an unambiguous assignment of the three $^{195}Pt$ signals. The absence of any cross peaks between the (1,1) and (2,2) linkage isomer signals indicated that the 1,2 shifts of each ring occurred independently and not in a concerted manner. Integrations of the spectra yielded accurate values for the solution populations of the linkage isomers (Table 9).

The acquisition of an informative $^{195}Pt$ two-dimensional EXSY spectrum of $[PtIMe_3(4Me\text{-}pydz)_2]$ was not immediately successful and several experiments were performed with successively shorter ranges of evolution times, D0, before any signals were observed. This was achieved by steadily increasing the spectral width to 2252 (F2) and 1126 Hz (F1) since the evolution time, D0, and its range of variation is inversely related

**Table 8** $^1$H NMR data (303 K)* for complexes $[ReX(CO)_3(pydz)_2]$ (X = Cl, Br or I)

| X | Solvent | $\delta_A(J_{AB},J_{AC},J_{AD})$ | $\delta_B(J_{BC},J_{BD})$ | $\delta_C(J_{CD})$ | $\delta_D$ |
|---|---|---|---|---|---|
| Cl | $CDCl_3$ | 9.61 | 9.02 | 7.66 | 7.64 |
| | | (1.28, 4.22, 2.70) | (2.66, 4.09) | (3.60) | |
| Br | $(CDCl_2)_2$ | 9.68 | 9.02 | 7.65 | 7.63 |
| | | (1.16, 4.21, 2.82) | (2.89, 4.11) | (3.59) | |
| I | $(CDCl_2)_2$ | 9.90 | 9.02 | 7.63 | 7.62 |
| | | (1.21, 4.21, 2.87) | (2.95, 4.13) | (3.60) | |

* Chemical shifts ($\delta$) relative to $SiMe_4$ as an internal standard; scalar couplings $J_{ij}$ in Hz.

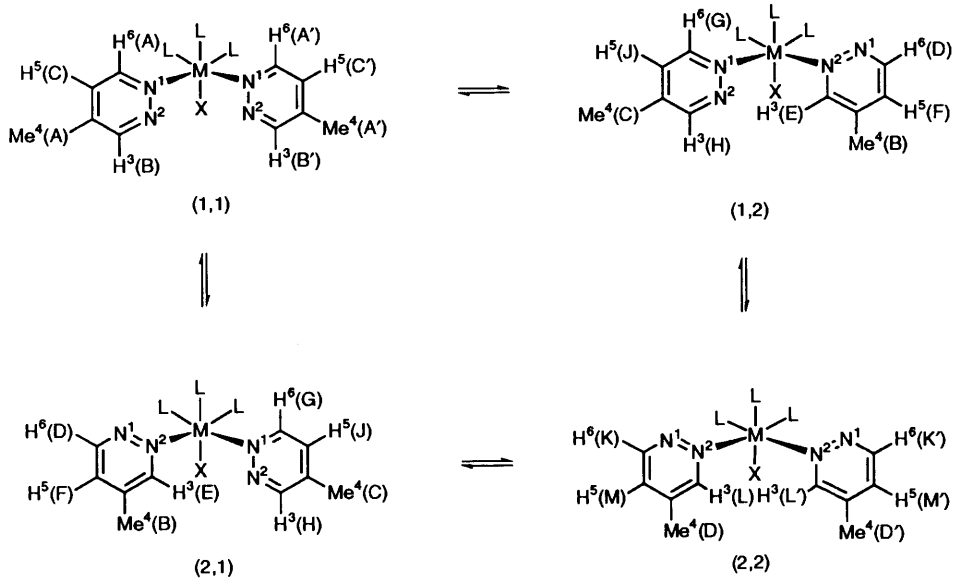


**Fig. 6** The linkage isomers of the complexes *fac*-$[MXL_3(4Me\text{-}pydz)_2]$ showing the hydrogen labelling. Note that isomers (1,2) and (2,1) are enantiomers. Non-concerted 1,2-M–N shifts cause the exchanges shown. The structures shown are arbitrarily chosen rotamers from the total set arising from rapid M–N bond rotations

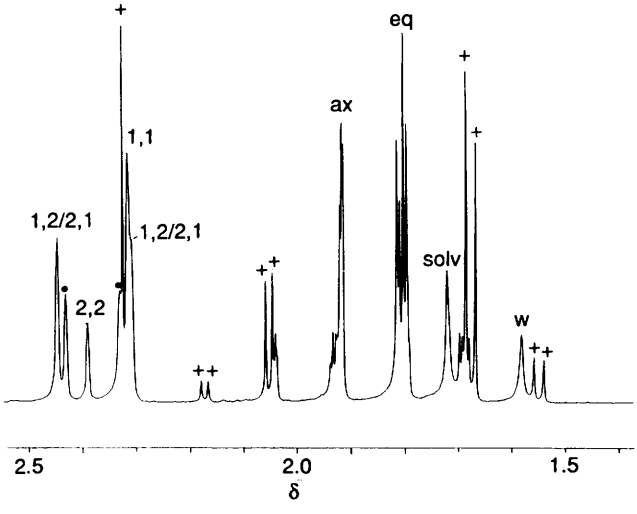


**Fig. 7** The $^1$H NMR spectrum of $[PtClMe_3(4Me\text{-}pydz)_2]$ in $CD_2Cl_2$–$C_6D_6$ (*ca.* 40:60 v/v) at 278 K showing the methyl signals due to the major and minor complex species. Main signal assignments given in Table 9. Additional signals are labelled + and •; solv = solvent, w = water

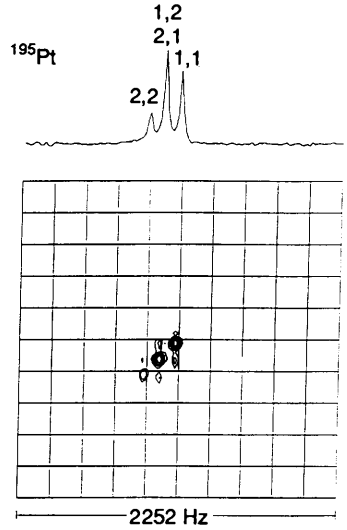


**Fig. 8** The $^{195}$Pt two-dimensional EXSY NMR spectrum of $[PtIMe_3(4Me\text{-}pydz)_2]$ at 308 K in $CDCl_3$ showing exchange between the (1,2)/(2,1) enantiomeric pair of isomers and the (1,1) and (2,2) isomers

to the spectral width parameter. It was thought that the experimental problem was associated with abnormally short spin–lattice relaxation times of $^{195}$Pt in these complex species, so $T_1$ data were measured by the standard inversion recovery method.[25] The $T_1$ values obtained, namely 0.63 (1,1 complex), 0.58 (1,2/2,1) and 0.55 s (2,2) were not especially short, being within the range noted previously.[26] It would appear therefore that the loss of signal intensity associated with longer D0 values was due to rapid spin–spin relaxation of the $^{195}$Pt nuclei. This is reflected in the breadth of the $^{195}$Pt signals even in the absence of any exchange broadening. For example, at 0 °C, the widths at half maximum height are *ca.* 8.6 Hz, giving a spin–spin relaxation time $T_2$* value of 37 ms. Such efficient relaxation is probably *via* scalar coupling of the directly bonded quadrupolar $^{14}$N nuclei.

**Table 9** Static $^1H$ and $^{195}Pt$ NMR parameters for the complexes $[PtXMe_3(4Me\text{-}pydz)_2]$ (X = Cl, Br or I)

| X | Solvent | T/K | Isomer | Population (%) | δ(Pt–$CH_3$)[a,b] | δ(Me-4)[a,c] |
|---|---|---|---|---|---|---|
| Cl | $CD_2Cl_2$–$C_6D_6$ | 278 | (1,1) | 38.3 | 1.824(eq) 1.933(ax) | 2.32(1) |
| | | | (1,2)/(2,1) | 25.0 | 1.817(eq) 1.930(ax) | 2.31(1) |
| | | | | 25.0 | 1.836(eq) | 2.45(2) |
| | | | (2,2) | 11.7 | 1.829(eq) 1.935(ax) | 2.39(2) |
| | | | | | δ(Pt)[d] | |
| Br | $(CDCl_2)_2$ | 273 | (1,1) | 38.1 | 2149.9 | |
| | | | (1,2)/(2,1) | 23.0 | 2151.5 | |
| | | | (2,2) | 15.9 | 2152.7 | |
| I | $(CDCl_2)_2$ | 273 | (1,1) | 38.3 | 2017.1 | |
| | | | (1,2)/(2,1) | 23.55 | 2018.4 | |
| | | | (2,2) | 14.6 | 2019.4 | |

[a] Chemical shifts quoted relative to $SiMe_4$ as an internal standard. [b] ax = Axial, eq = equatorial. [c] (1) = co-ordinated *via* $N^1$, (2) = co-ordinated *via* $N^2$. [d] Chemical shifts quoted relative to $\Xi(^{195}Pt) = 21.4$ MHz.

**Table 10** Static $^1H$ NMR data of $[ReX(CO)_3(4Me\text{-}pydz)_2]$ complexes in solution

| | | δ($^1H$)[a] | | | | | | | | | | | | | | |
|---|---|---|---|---|---|---|---|---|---|---|---|---|---|---|---|---|
| | | Aromatic hydrogens | | | | | | | | | | | | Methyl hydrogens | | |
| X | Solvent | A/A' | B/B' | C/C' | D | E | F | G | H | J | K/K' | L/L' | M/M' | A/A' | B | C | D/D' |
| Br | $C_6D_6$ | 9.55 | ≈7.9 | 5.97 | ≈7.9 | 9.78 | 5.83 | 9.52 | ≈7.9 | 5.94 | ≈7.9 | 9.74 | 5.81 | 1.15 | 1.21 | 1.13 | 1.18 |
| I | $C_6D_5CD_3$ | 9.56 | ≈8.0 | 6.22 | ≈8.0 | 9.77 | 6.10 | 9.53 | ≈8.0 | 6.19 | ≈8.0 | 9.73 | 6.12 | 1.42 | 1.45 | 1.44 | 1.40 |
| | | Scalar coupling constants J/Hz | | | | | | | | | | | | | | |
| | | AB/A'B' | BC/B'C' | AC/A'C' | DE | DF | EF | GH | HJ | GJ | KL/K'L' | KM/K'M' | LM/L'M' | | | |
| Br | $C_6D_6$ | 1.09 | 2.61 | 5.92 | 1.16 | 2.59 | 2.04 | 1.13 | 2.52 | 5.98 | 1.14 | 2.56 | 2.13 | | | |
| I | $C_6D_5CD_3$ | *b* | 1.95 | 5.95 | *b* | *b* | *b* | *b* | 1.90 | 5.60 | *b* | *b* | *b* | | | |

[a] Relative to $SiMe_4$ as an internal standard. [b] Values unable to be measured accurately due to limited spectral resolution.

The small chemical shift spread of the $^{195}Pt$ signals enabled standard bandshape analysis to be carried out at different temperatures. Solutions of X = Br and X = I complexes in $(CHCl_2)_2$–$(CDCl_2)_2$ were heated in the temperature range 0–110 °C. The expected broadening and eventual coalescence of the bands occurred and total bandshape analysis was applied to the spectra. The spin problem is of the type (1). There are two

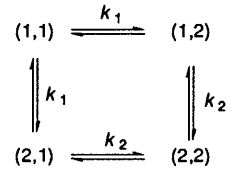


(1)

independent rate constants, namely, $k_1$ for (1,1) ⟶ (1,2)/(2,1) exchange and $k_2$ for (1,2)/(2,1) ⟶ (2,2) exchange, and the $^{195}Pt$ spectra were fitted on this basis. The case of X = I is illustrated in Fig. 9. Simultaneous 1,2 shifts of both ligands were assumed to be of negligible rate in accordance with a non-concerted shift mechanism. Although quantitative dynamic NMR studies involving $^{195}Pt$ spectra have been reported previously,[27–29] this would appear to be the first example of a *total* bandshape analysis of variable-temperature $^{195}Pt$ spectra. The method is normally impractical on account of the very large chemical shift dispersion of most $^{195}Pt$ spectra, which results in them possessing little dynamic information.

(*iv*) $[ReX(CO)_3(4Me\text{-}pydz)_2]$ (X = Br *or* I).—These complexes were isolated and their $^1H$ NMR spectra obtained in $C_6D_6$ or $C_6D_5CD_3$ solutions. The static NMR data for both complexes are given in Table 10. The sample of the iodo complex exhibited weak, extra signals in its $^1H$ spectrum which indicated the presence of an additional complex species, possibly one involving bridging 4-methylpyridazine, but it was not easy to rationalise the somewhat higher than expected values for C, H and N elemental analyses of the samples.

The bromo complex gave a very informative $^1H$ spectrum that was consistent with the structure $[ReBr(CO)_3(4Me\text{-}pydz)_2]$ existing as a mixture of (1,1), (1,2), (2,1) and (2,2) linkage isomers. Relative populations of these were 37.8, 23.8, 23.8 and 14.7% respectively. Spectra recorded in aromatic solvents (*e.g.* $C_6D_6$ or $C_6D_5CD_3$) provided the greatest distinction between solution isomers. The spectrum in $C_6D_6$ is shown in Fig. 10. The four methyl signals labelled A–D (Fig. 6) are clearly resolved and assigned as shown, B and C having equal intensity as they belong to the same (1,2) or (2,1) linkage isomers. The aromatic ring hydrogen signals fall into five distinct groups. The highest frequency signals (E,L,L') are due to 3-position hydrogens *ortho* to both a co-ordinated nitrogen and the methyl substituent. The next group of signals (A,A',G) arises from the 6-position hydrogens *ortho* to a co-ordinated nitrogen. The middle group (B,B',D,H,K,K') is due to hydrogens *ortho* to an unco-ordinated nitrogen. The next group (C,C',J) arises from hydrogens *meta* to a co-ordinated nitrogen, and the lowest frequency group (F,M,M') represents hydrogens *meta* to an unco-ordinated nitrogen.

On warming the complex, the 1,2-fluxional shifts cause exchange between the aromatic hydrogens according to (2) and exchange between the methyls according to (3). Since no scalar couplings occur between ligand rings the spin problem reduces to (4).

The kinetics were followed by two-dimensional EXSY at temperatures of 343 and 356 K and by one-dimensional

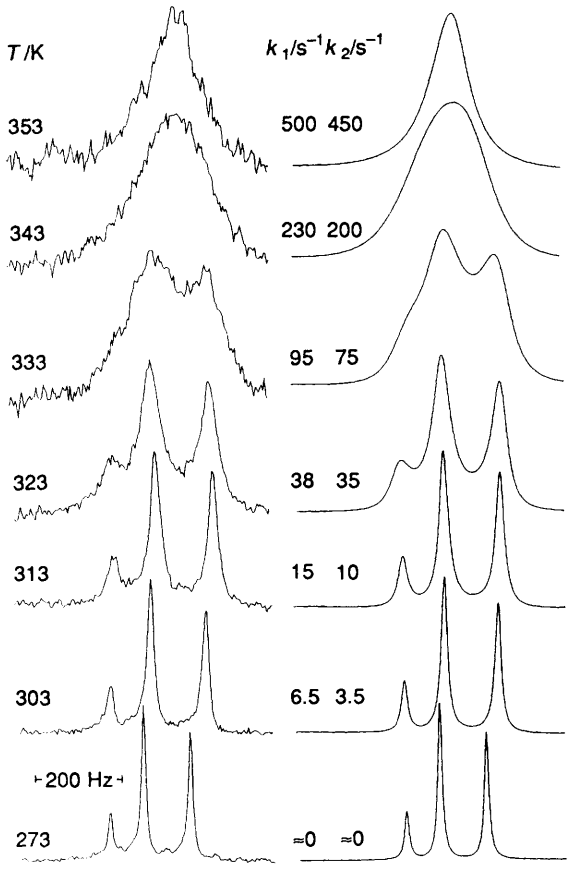


**Fig. 9** Variable-temperature $^{195}Pt$ NMR spectra of $[PtIMe_3(4Me\text{-}pydz)_2]$. The 'best-fit' computer simulated spectra are shown alongside with the rate constants $k_1$ and $k_2$ for the two exchange pathways

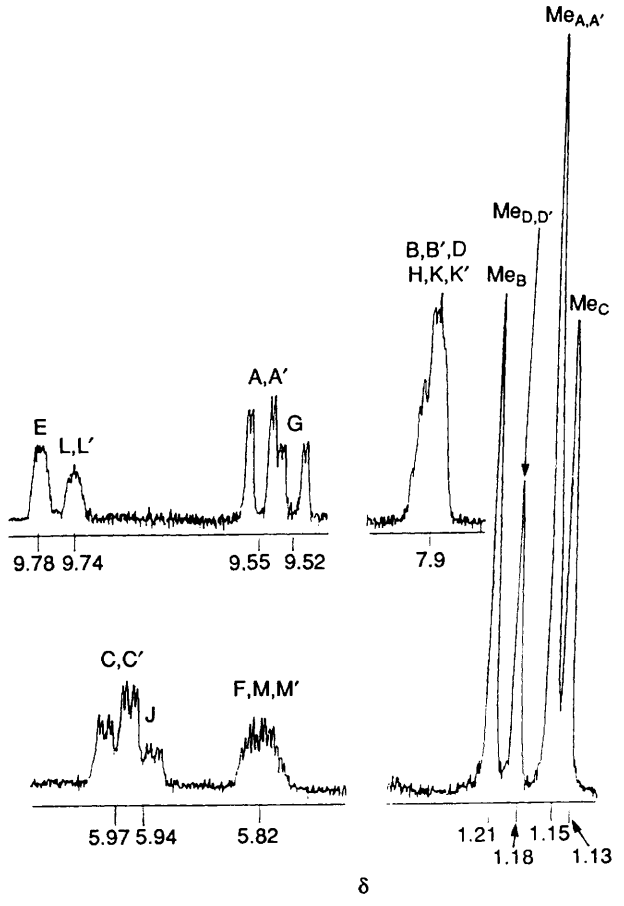


**Fig. 10** The $^1H$ NMR spectrum of $[ReBr(CO)_3(4Me\text{-}pydz)_2]$ at 298 K in $C_6D_6$ showing signals due to the mixture of all linkage isomers. Signal labels refer to Fig. 6

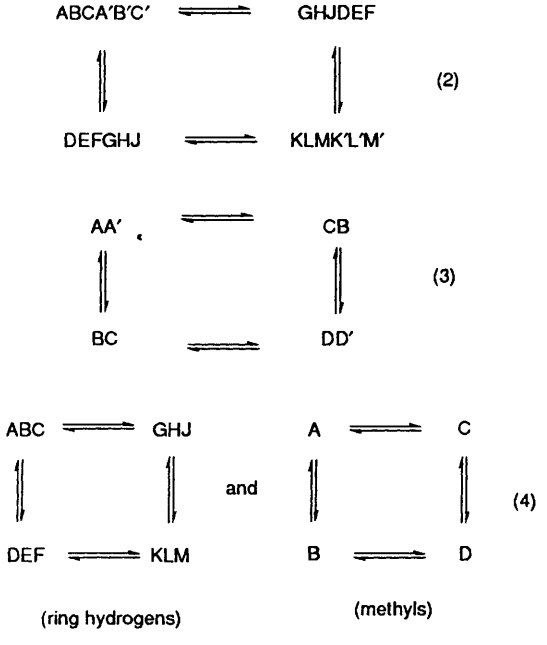


bandshape analysis in the range 363–383 K. The two-dimensional EXSY spectrum of the methyl signals at 356 K is shown in Fig. 11. Good fittings were achieved on the basis of two non-zero constants, $k_1$ and $k_2$, as defined for the $Pt^{IV}$ complexes. Activation energy parameters for the 1,2 shift are given in Table 11 with the data for the analogous $[PtXMe_3(4Me\text{-}pydz)_2]$ complexes.

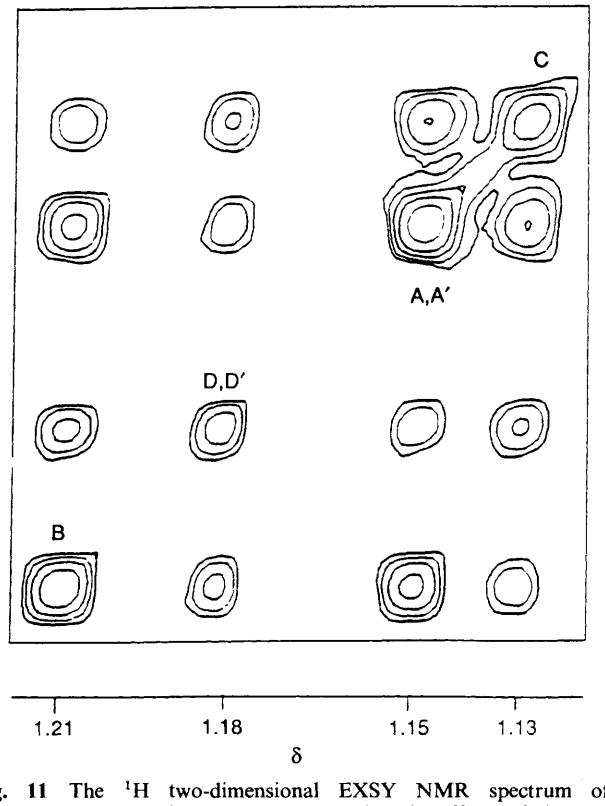


**Fig. 11** The $^1H$ two-dimensional EXSY NMR spectrum of $[ReBr(CO)_3(4Me\text{-}pydz)_2]$ at 356 K showing the effects of the 1,2-metallotropic shifts on the methyl signals

**Table 11** Eyring activation parameters[a] for the complexes $[PtXMe_3(4Me\text{-}pydz)_2]$ and $[ReX(CO)_3(4Me\text{-}pydz)_2]$

| Complex | Process | $\Delta H^{\ddagger}$/kJ mol$^{-1}$ | $\Delta S^{\ddagger}$/J K$^{-1}$ mol$^{-1}$ | $\Delta G^{\ddagger}$/kJ mol$^{-1}$ |
|---|---|---|---|---|
| $[PtClMe_3(4Me\text{-}pydz)_2]$ | | — | — | 74.4[b] |
| $[PrBrMe_3(4Me\text{-}pydz)_2]$ | (1,2) ⟶ (1,2) | 62.8 ± 2.4 | −21.8 ± 7.2 | 69.3 ± 0.2 |
| | (1,2) ⟶ (2,2) | 72.6 ± 3.3 | 6.3 ± 9.8 | 70.7 ± 0.4 |
| $[PtIMe_3(4Me\text{-}pydz)_2]$ | (1,1) ⟶ (1,2) | 76.0 ± 1.0 | 20.2 ± 3.2 | 69.9 ± 0.1 |
| | (1,2) ⟶ (2,2) | 91.7 ± 4.3 | 65.6 ± 13.4 | 72.1 ± 0.3 |
| $[ReBr(CO)_3(4Me\text{-}pydz)_2]$ | (1,1) ⟶ (1,2) | 112.8 ± 2.3 | 68.2 ± 6.3 | 92.5 ± 0.4 |
| | (1,2) ⟶ (2,2) | 101.3 ± 4.9 | 39.4 ± 13.4 | 89.6 ± 0.9 |
| $[ReI(CO)_3(4Me\text{-}pydz)_2]$ | | — | — | ≈86[c] |

[a] At 298.15 K. [b] Approximate value calculated from a single two-dimensional EXSY spectrum at 295 K. [c] Approximate value based on band coalescence at 383 K.

The complex $[ReI(CO)_3(4Me\text{-}pydz)_2]$ was somewhat impure (Table 2) and produced less informative $^1H$ NMR spectra. Evidence of the four linkage isomers was obtained, however, with relative populations of 32 (1,1), 24 (1,2), 24 (2,1) and 20% (2,2). Variable-temperature $^1H$ NMR spectra indicated the presence of the 1,2-shift process and an approximate value for the energy barrier ($\Delta G^{\ddagger}$) was calculated by the band coalescence method (Table 11).

*Activation Energies and Mechanisms of the* 1,2-*Metallotropic Shift.*—An examination of the activation energy data for the 1,2-metallotropic shift in the *fac*-octahedral $Pt^{IV}$ and $Re^{I}$ complexes (Tables 5 and 11) reveals the following points. (*i*) Energy barriers [$\Delta G^{\ddagger}$ (298.15 K)] for the $Pt^{IV}$ complexes lie in the range 69–74 kJ mol$^{-1}$ and for the $Re^{I}$ complexes in the higher range, 85–93 kJ mol$^{-1}$, presumably reflecting the relative strengths of the Pt–N and Re–N bonds. A similar trend has recently been noted in the energies of 1,4-M–N fluxions in bidentate chelate complexes of 2,2′:6′,2″-terpyridine, although here the absolute magnitudes of the energies were significantly lower.[30] (*ii*) There is no consistent halogen dependence of the energy barriers for either series of metal complexes. (*iii*) The consequences of methyl substitution at the 4 position of the pyridazine are three-fold. (*a*) Solution populations of the four linkage isomers are affected such that the (1,1) isomer is favoured in all cases, the order being (1,1) > (1,2) = (2,1) > (2,2). Halogen dependence of these populations is very slight in both series of complexes and shows no regular trends. (*b*) Co-ordination at $N^1$ (Fig. 6) might be expected to be electronically favoured by the inductive effect of the methyl group. However, methyl substitution leads to no increase in $\Delta G^{\ddagger}$ values for the (1,1) ⟶ (1,2)/(2,1) exchange suggesting that there is no change in the ground-state energy of the (1,1) linkage isomer. This is consistent with earlier studies on 4-methylpyridazine methiodide compounds where equal amounts of both quaternary salts $[\overline{CHC(Me)CHCHN(Me)N}]^+I^-$ and $[\overline{CHC(Me)CHCHNNMe}]^+I^-$ were detected in solution.[31] (*c*) The $\Delta G^{\ddagger}$ values for the (1,2)/(2,1) ⟶ (2,2) process reveal subtle differences arising from the steric effects of 4-methyl substitution. For the $Pt^{IV}$ series, a small increase is observed. This is attributed to the increased steric interaction between the ligand methyls and the $PtXMe_3$ moiety in the transition state. Conversely, the small decrease in $\Delta G^{\ddagger}$ values for the $Re^{I}$ complexes is thought to reflect the smaller steric interactions between the ligand methyls and the less bulky $ReX(CO)_3$ group in the transition state.

The nature of the transition state associated with these 1,2-M–N shifts in pyridazine complexes has been discussed in the case of $[M(CO)_5(pydz)]$ complexes.[10] Some theoretical calculations[6] suggest a bound, bidentate, 20-electron intermediate species associated with a sliding and rotation of the ligand such that the M–N distances in the intermediate are equal to the bonding distance in the monodentate species. In the case of $[Cr(CO)_5(pydz)]$ other workers[5] have predicted theoretically that the transition state is characterised by very long Cr–N bonds suggesting substantial dissociative character rather than being a π-bonded intermediate. This prediction was supported experimentally by the sizeably positive activation entropies, $\Delta S^{\ddagger}$, arising from dynamic NMR studies of $[W(CO)_5(pydz)]$. In this present work, $\Delta S^{\ddagger}$ values associated with the 1,2 shift are again significantly positive in most cases, supporting an intermediate structure with some dissociative character. However, in view of the considerable variations in the magnitude of these $\Delta S^{\ddagger}$ values and difficulties in their precise estimation in the present work, caution must be exercised in drawing any firm structural significance from them. Indeed, we are inclined to the view that in these complexes the intermediates are rather less dissociative and possess rather more π-bonded character than the $[M(CO)_5(pydz)]$ (M = Cr or W) complexes.

## Acknowledgements

We thank the SERC for use of the mass spectrometry service at the University College of Swansea and support of the X-ray work at the University College of Cardiff. We are grateful to the SERC and the University of Exeter for research studentships (to E. S. B. and P. J. H.). We are also grateful to Dr. K. Kite for useful discussions.

## References

1 J. Reedijk, in *Comprehensive Coordination Chemistry*, eds. G. Wilkinson, R. D. Gillard and J. A. McCleverty, Pergamon Press, Oxford, 1987, vol. 2, p. 73 and following.
2 M. Herberhold, W. Golla and K. Leonhard, *Chem. Ber.*, 1974, **107**, 3209.
3 E. C. Constable and P. J. Steel, *Coord. Chem. Rev.*, 1989, **93**, 205.
4 P. J. Steel, *Coord. Chem. Rev.*, 1990, **106**, 227.
5 S-K. Kang, T. A. Albright and C. Mealli, *Inorg. Chem.*, 1987, **26**, 3158.
6 S. Alvarez, M-J. Bermejo and J. Vinaixa, *J. Am. Chem. Soc.*, 1987, **109**, 5316.
7 S. S. Eaton, G. R. Eaton and R. H. Holm, *J. Organomet. Chem.*, 1972, **39**, 179.
8 M-J. Bermejo, J-I. Ruiz and J. Vinaixa, *Transition Met. Chem.*, 1987, **12**, 245.
9 K. R. Dixon, *Inorg. Chem.*, 1977, **16**, 2618.
10 E. W. Abel, E. S. Blackwall, K. G. Orrell and V. Šik, *J. Organomet. Chem.*, in the press.
11 J. C. Baldwin and W. C. Kaska, *Inorg. Chem.*, 1975, **14**, 2020.
12 D. H. Goldsworthy, Ph.D. Thesis, University of Exeter, 1980.
13 S. P. Schmidt, W. C. Trogler and F. Basolo, *Inorg. Synth.*, 1979, **28**, 160.
14 D. D. Perrin and W. L. F. Armarego, *Purification of Laboratory Chemicals*, Pergamon Press, Oxford, 1988.
15 D. F. Shriver, *Manipulation of Air-Sensitive Compounds*, McGraw-Hill, New York, 1969.
16 E. W. Abel, G. B. Hargreaves and G. Wilkinson, *J. Chem. Soc.*, 1958, 3149.
17 D. A. Kleier and G. Binsch, Program DNMR3, Quantum Chemistry Program Exchange, Indiana University, 1970.

18 E. W. Abel, T. P. J. Coston, K. G. Orrell, V. Šik and D. Stephenson, *J. Magn. Reson.*, 1986, **70**, 34.
19 A. A. Danopoulos, M. B. Hursthouse, B. Hussain-Bates and G. Wilkinson, *J. Chem. Soc., Dalton Trans.*, 1991, 1855.
20 G. M. Sheldrick, SHELX L-93, Program for Crystal Structure Refinement, *J. Appl. Crystallogr.*, in the press; DIFABS, N. P. C. Walker and D. Stuart, *Acta. Crystallogr. Sect. A*, 1983, **39**, 158.
21 D. E. Clegg, J. R. Hall and G. A. Swile, *J. Organomet. Chem.*, 1972, **38**, 403.
22 J. R. Hall, *Essays in Structural Chemistry*, eds. A. J. Downs, D. A. Long and L. A. K. Staveley, Macmillan, London, 1971, p. 433.
23 A. Psaila, Ph.D. Thesis, University of Exeter, 1977.
24 E. W. Abel, S. K. Bhargava and K. G. Orrell, *Prog. Inorg. Chem.*, 1984, **32**, 1.
25 R. K. Harris, *Nuclear Magnetic Resonance Spectroscopy*, Pitman, London, 1983, p. 81.
26 P. S. Pregosin, *Annu. Ref. NMR Spectrosc.*, 1986, **17**, 285.
27 K. G. Orrell, V. Šik, C. H. Brubaker and B. J. McCulloch, *J. Organomet. Chem.*, 1984, **276**, 267.
28 D. D. Gummin, E. M. A. Ratilla and N. M. Kostic, *Inorg. Chem.*, 1986, **25**, 2429.
29 J. A. Galbraith, K. A. Menzel, E. M. A. Ratilla and N. M. Kostic, *Inorg. Chem.*, 1987, **26**, 2073.
30 E. W. Abel, V. S. Dimitrov, N. J. Long, K. G. Orrell, A. G. Osborne, H. M. Pain, V. Šik, M. B. Hursthouse and M. A. Mazid, *J. Chem. Soc., Dalton Trans.*, 1993, 597.
31 M. S. Bale, A. B. Simmonds and W. F. Trager, *J. Chem. Soc. B*, 1966, 867.

*Received* 26*th August* 1993; *Paper* 3/05158G